Journal of Rehabilitation in Civil Engineering 7-4 (2019) 168-179

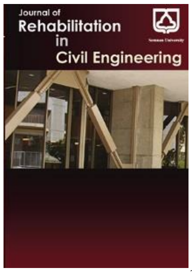

journal homepage: http://civiljournal.semnan.ac.ir/

Effect of Degradation on Collapse Margin Ratio of Steel Moment Frames

S. Bazvand[1], E. Darvishan[2*], G. Ghodrati Amiri[3]

1. M.Sc. of Earthquake Engineering, Faculty of Civil Eng., Shahre Kord Branch, Islamic Azad University, Shahre Kord, Iran
2. Assistant Professor, Department of Civil Engineering, Roudehen Branch, Islamic Azad University, Roudehen, Iran
3. Professor, Faculty of Civil Engineering, Iran University of Science and Technology, Tehran, Iran

Corresponding author: *darvishan@riau.ac.ir*

ARTICLE INFO

Article history:
Received: 20 November 2017
Accepted: 08 December 2018

Keywords:
Degrading Behavior,
Collapse Capacity,
Strength Degradation,
FEMA-P695,
Steel Moment Frame.

ABSTRACT

Although several studies have investigated the effect of degradation on the behavior of structures, inspections on collapse margin ratios are rare in the literature. In this study, the effect of strength and stiffness degradation on collapse capacity of steel moment frames is inquired. The aim is to determine margin of safety against collapse applying a probabilistic approach. To this end, 14 moment frames are designed including 4 long period and 3 short period models with 5 and 8m bay length. These buildings are representative of common office and residential buildings built in cities. Also, they are designed in consonance with ASCE7-05 specifications. In the first stage, effective seismic parameters are calculated using a pushover analysis. In the second stage, collapse performance levels are determined using incremental dynamic analysis by considering seismic excitation uncertainties. Results reveal that the overstrength factor that is recommended by ASCE code is not always conservative. Overall, structures designed with common building codes show acceptable margin of safety against collapse.

1. Introduction

Preventing collapse of structures has always been a concern for earthquake engineers. Collapse means that the structure is no longer able to tolerate gravity loads during a seismic action. For this reason, numerous methods are introduced to understand and evaluate mechanism of collapse. Some of researchers investigated the P-Δ effect on collapse capacity of structures, while others focused on the effect of strength and stiffness degradation on severity of damage [1-6]. Regardless of which, in recent years the role of strength and stiffness degradation has attracted more attention.

Rahnama and Krawinkler [7] indicated that strength degradation in nonlinear SDOF systems increases post-elastic displacements

DOI: 10.22075/JRCE.2018.12535.1240

and therefore leads to considerably higher ductility demands. Miranda and Akkar [8] investigated the minimum lateral strength required to prevent collapse of degrading SDOF systems. Their studies revealed that strength and stiffness degradation has a major effect on earthquake induced

Table 1. Structures specifications and performance groups.

Group No.	T	No. of stories	Design parameters							
			(gravity loads	Bay length (m)	Seismic parameters					$S_{MT}(T_1)$(g)
					SDC	R	T_a (sec)	T_1	C_s	
Performance group A (5m bay length, short period)										
01 – A	short	1	ordinary	5	D_{max}	8	0.18	0.31	0.1225	1.5
02 – A		2	ordinary	5	D_{max}	8	0.32	0.56	0.1225	1.5
03 – A		3	ordinary	5	D_{max}	8	0.44	0.69	0.1090	1.3
Performance group B (5m bay length, long period)										
06 – B	long	6	ordinary	5	D_{max}	8	0.77	1.03	0.073	0.87
09 – B		9	ordinary	5	D_{max}	8	1.06	1.43	0.053	0.63
12 – B		12	ordinary	5	D_{max}	8	1.34	1.60	0.047	0.56
15 – B		15	ordinary	5	D_{max}	8	1.60	1.98	0.038	0.45
Performance group C (8m bay length, short period)										
01 – C	short	1	ordinary	8	D_{max}	8	0.18	0.28	0.1225	1.5
02 – C		2	ordinary	8	D_{max}	8	0.32	0.45	0.1225	1.5
03 – C		3	ordinary	8	D_{max}	8	0.44	0.56	0.1225	1.5
Performance group D (8m bay length, long period)										
06 – D	long	6	ordinary	8	D_{max}	8	0.77	0.88	0.085	1.02
09 – D		9	ordinary	8	D_{max}	8	1.06	1.37	0.058	0.66
12 – D		12	ordinary	8	D_{max}	8	1.34	1.52	0.049	0.59
15 – D		15	ordinary	8	D_{max}	8	1.60	1.79	0.043	0.50

displacements. Song and Pinchera [9] inspected the role of strength and stiffness degradation on maximum response of degrading systems. They concluded that the displacement caused by earthquake, specially, in short period structures, can result in up to two times higher displacement demands in degrading systems in comparison to nondegrading ones. Ibarra et al. [10] conducted a comprehensive study on strength and stiffness degradation and their effect on amplification of dynamic instability of structures. These studies were later followed by Ibarra et al. [11] and Ibarra and Krawinkler [12] as well.

Although numerous studies are conducted on the effect of degradation on seismic behavior of the structures, margins of safety of such structures against marginal performance levels is not well understood. Accordingly, the aim of this study is to investigate the effect of stiffness and strength degradations on collapse margin ratios of steel moment frames with different configurations applying a probabilistic approach. To this end, a relatively widespread range of steel moment frames with 1-, 2-, 3-, 6-, 9-, 12- and 15-story structures with 5 and 8 m bay length is considered which includes total of 14 structures. Nonlinear static and dynamic analyses are carried out. Finally, margin of safety of the structures against collapse is calculated applying FEMA-P695 methodology [13].

2. Design and Modeling of Structures

In this study, steel moment frame structures are selected in a way that they are representative of common residential and office buildings built in cities. On this basis, 1-, 2-, 3-, 6-, 9-, 12- and 15- story structures are deliberated.

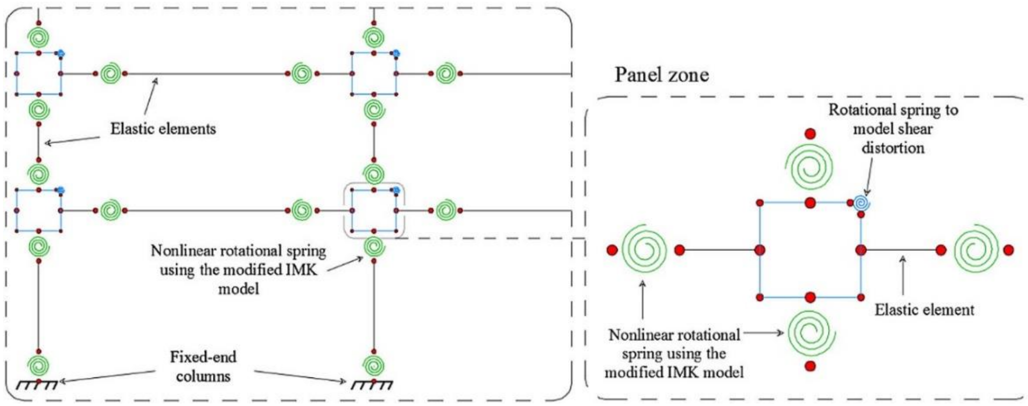

Fig. 1. connection an panel zone modeling details [20].

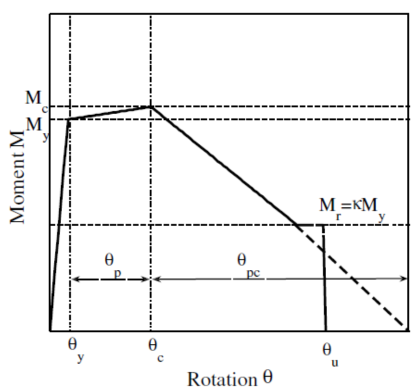

Fig. 2. General moment-rotation behavior [17].

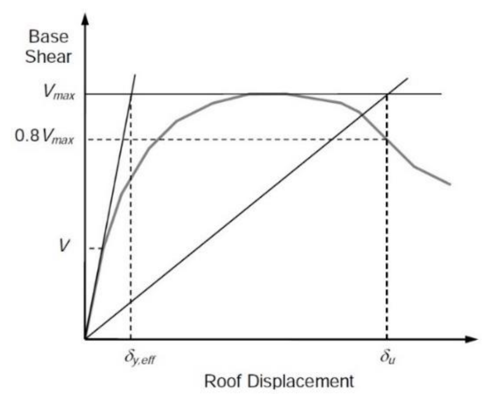

Fig 3. Calculation of maximum displacement capacity [13].

All the structures have 3 bays. Two types of structures are designed with 5 and 8 bay length. Buildings are designed confirming to ASCE/SEI7-05 [14] code. Seismic design parameters including response modification factor (R), overstrength factor (Ω_0), and deflection amplification factor (C_d) are selected as 8, 2.7, and 5.5, respectively. Dead and live loads of stories are considered as 600 kg/m^2 and 200 kg/m^2 which are distributed pursuant to the bay`s tributary load area. It is assumed that the buildings are located in an area with very high seismicity and soil type III [15]. Frames are regular in plan and elevation. Therefore, 2D models are utilized for analysis. Table 1 lists the buildings specifications, performance groups, and index archetypes.

Modeling and analysis is carried out applying OpenSEES [16] software. Concentrated plasticity is used to model nonlinear behavior of frame members. For this purpose, beam-column members are modeled as elastic elements. Nonlinear springs are placed at the end of members to model nonlinearity. ‘Bilin’ material [17] is used to capture moment-rotation relationship. This material can model hysteresis behavior with stiffness and strength degradation. Nonlinear parameters are designated in consonance with Lignos and Krawinkler [18] suggestion (Fig. 2). According to the figure, M_y and M_p are

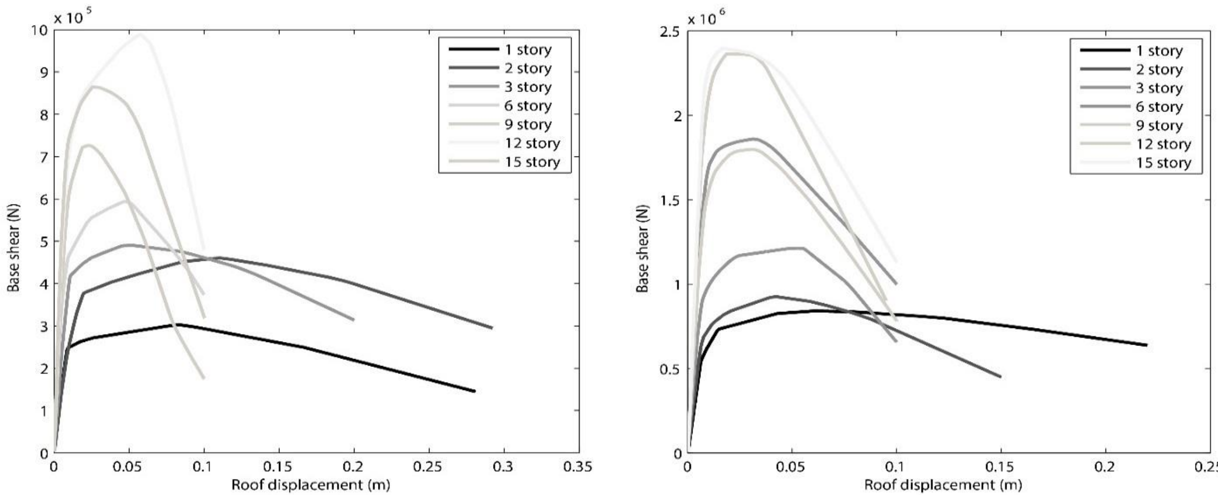

a) structures with 5m bay length b) structures with 8m bay length

Fig. 4. Comparison of pushover curves.

calculated based on the section properties and θ_y, θ_p, and θ_{pc} are estimated using Eq. 1

$$\theta_p = 0/0865*\left(\frac{h}{t_w}\right)^{-0/365}*\left(\frac{b_f}{2*t_f}\right)^{-0/140}*\left(\frac{L}{d}\right)^{0/340}*\left(\frac{c_{unit}^{1}*d}{533}\right)^{-0/721}*\left(\frac{c_{unit}^{2}*F_y}{355}\right)^{-0/230}$$

$$\theta_{pc} = 5/63*\left(\frac{h}{t_w}\right)^{-0/565}*\left(\frac{b_f}{2*t_f}\right)^{-0/800}*\left(\frac{c_{unit}^{1}*d}{533}\right)^{-0/280}*\left(\frac{c_{unit}^{2}*F_y}{355}\right)^{-0/430}$$

$$\Lambda = \frac{E_u}{M_y} = 563*\left(\frac{h}{t_w}\right)^{-\frac{1}{26}}*\left(\frac{b_f}{2*t_f}\right)^{-\frac{0}{525}}*\left(\frac{L_b}{r_y}\right)^{-\frac{1}{26}}*\left(\frac{c_{unit}^{2}*F_y}{355}\right)^{-0/291} \quad (1)$$

Recent studies indicate that modeling of panel zone in the analysis can strongly affect the structural behavior. It reduces lateral stiffness and can cause intensification of drift demands [19]. Accordingly, Panel zone is modeled here. As depicted in Fig. 1, panel zone includes 8 rigid elements. These elements are connected together with joints at three corners. In the fourth corner a nonlinear spring is added to capture nonlinear behavior of the panel zone. ‘hysteresis’ material is applied for the spring. The moment-rotation behavior of the panel zone is adopted from Gupta and Krawinkler [20] using a trilinear curve. Ground motion records are selected from FEMA-P695 data set. This record set contains 22 pair of far field ground motion records.

3. Static Pushover Analysis

According to FEMA-P695, overstrength factor (Ω_0) and period-based ductility (μ_T) are calculated by nonlinear static (pushover) analysis. The analysis is confirming to the first mode of vibration. First, corresponding load combination is determined for gravity loads. Second, structure weight (W) and earthquake base shear (V) are calculated. The base shear is distributed in height (V_x) according to Eq. 2

$$V_x = V \times \frac{m_x \Phi_{l,x}}{\sum_{X=1}^{n} m_x \Phi_{l,x}} \quad (2)$$

Where m_x is mass at level x and $\Phi_{l,x}$ is the mode shape vector at level x. Figure 3 illustrates an idealized pushover curve. In the figure, V_{max}, δ_u, and $\delta_{y,eff}$ are maximum base shear capacity, maximum displacement capacity, and equivalent displacement of maximum base shear in elastic case, respectively.

In FEMA-P695 methodology, maximum displacement capacity (δ_u) corresponds to a displacement in which base shear capacity drops to 80% of maximum base shear capacity (V_{max}). Overstrength factor (Ω) is defined as the ratio of maximum base shear (V_{max}) and the base shear calculated from code provisions

$$\Omega = \frac{V_{Max}}{V} \quad (3)$$

Also, period-based ductility factor is defined as the ratio of maximum roof displacement capacity (δ_u) to the effective roof displacement ($\delta_{y,eff}$)

$$\mu_T = \frac{\delta_u}{\delta_{y,eff}} \quad (4)$$

effective roof displacement ($\delta_{y,eff}$) is determined by

$$\delta_{y,eff} = C_0 \frac{V_{max}}{W} \left[\frac{g}{4\pi 2}\right] (\max(T, T_1))^2 \quad (5)$$

Where $\frac{V_{max}}{W}$ is normalized maximum base shear, g is spectral acceleration, T is the first mode period, T_1 is the first mode period calculated from a eigen vector analysis, and C_0 is a factor which relates displacement correspond to first mode of vibration to roof displacement

$$C_0 = \Phi_{l,r} \times \frac{m_x \Phi_{l,x}}{\sum_{X=l}^{n} m_x \Phi_{l,x}^2} \quad (6)$$

Where m_x is mass at level *x*, $\Phi_{l,x}$($\Phi_{l,r}$) is the mode shape vector at level *x* (roof), and *n* is the number of stories.

Based on the methodology mentioned above, pushover analysis is carried out on the structures. A comparison of capacity curves is performed in Fig. 4. According to the figure, shorter structures are able to tolerate larger displacements. Moreover, structures with 5m bay length can reach larger base shear compared to structures with 8m bay length. However, 8m bay length structures show larger ductility. It is notable that modification in ductility is not tangible for structures with over 9 stories.

Table 2 presents the values of μ_T and Ω_0 calculated for the structures. It is obvious that overstrength factor (Ω_0) is extremely variable in short period structures, since it varies from 4.96 to 11.98. Furthermore, structures with 8m bay length demonstrate a wider range of Ω_0. Variations of Ω_0 in large period structures are limited between 5.3 and 8.46. The same trend is observed for μ_T. In general, ductility of short period structures is considerably larger than long period ones. According to the results, μ_T = 10 is suggested on average for the investigated structures.

Final results of pushover analysis for the 4 performance groups is provided in Table 3. It is note-worthy to mention that, μ_T provided in this table is the average of μ_T in each group. Ω_0 is provided in two cases: 1) maximum Ω_0 of the models in each performance group, 2) average Ω_0 of the models. FEMA-P695 uses the first approach to evaluate Ω_0. According

Table 2. Pushover analysis results of degrading systems.

Group No.	V design (C_W) (N)	$RDR_{y,eff}$	V_{max} (N)	RDR_u	Ω_0	μ_T	R
Group A							
01 – A	28286	0.0103	302432	0.175	10.70	17.00	8.00
02 – A	64875	0.0175	460190	0.2276	7.10	13.03	8.01
03 – A	92218	0.0129	490357	0.1527	5.54	11.84	7.95
Group B							
06 – B	116600	0.0094	594040	0.0799	4.82	8.46	7.94
09 – B	128400	0.0097	726020	0.0514	5.34	5.30	7.92
12 – B	137846	0.0105	988090	0.0805	6.10	7.70	7.94
15 – B	142702	0.0090	864385	0.0646	5.26	7.19	7.88
Group C							
01 – C	70215	0.0101	841508	0.0200	11.98	19.82	8.00
02 – C	157293	0.0091	925845	0.0972	5.88	10.65	8.02
03 – C	236552	0.0083	1213100	0.0790	4.96	9.52	8.03
Group D							
06 – D	279095	0.0083	1859222	0.0651	5.40	7.84	8.00
09 – D	603737	0.0094	1798828	0.0618	5.05	6.57	7.58
12 – D	328985	0.0118	2362985	0.0543	5.86	4.60	8.02
15 – D	340379	0.0084	2397139	0.0634	5.53	7.42	7.98

Table 3. Summary of pushover analysis for performance groups.

Performance group	$_T\mu$	$_0\Omega$	$_{ave}\Omega$
Group A	13.96	10.7	7.78
Group B	7.16	6.1	5.38
Group C	13.33	11.98	7.60
Group D	6.6	5.86	5.46

Table 4. Selected ground motion records for analysis**.**

No.	Earthquake			Recoding station	
	Mw	Year	Name	Name	Owner
1	6.7	1994	Northridge	Beverly Hills – Mulhol	USC
2	6.7	1994	Northridge	Canyon Country-WLC	USC
3	7.1	1999	Duzce, Turkey	Bolu	ERD
4	7.1	1999	Hector Mine	Hector	SCSN
5	6.5	1979	Imperial Valley	Delta	UNAMUCSD
6	6.5	1979	Imperial Valley	El Centro Array #11	USGS
7	6.9	1995	Kobe, Japan	Nishi-Akashi	CUE
8	6.9	1995	Kobe, Japan	Shin-Osaka	CUE
9	7.5	1999	Kocaeli, Turkey	Duzce	ERD
10	7.5	1999	Kocaeli, Turkey	Arcelik	KOERI
11	7.3	1992	Landers	Yermo Fire Station	CDMG
12	7.3	1992	Landers	Coolwater	SCE
13	6.9	1989	Loma Prieta	Capitola	CDMG
14	6.9	1989	Loma Prieta	Gilroy Array #3	CDMG
15	7.4	1990	Manjil, Iran	Abbar	BHRC
16	6.5	1987	Superstition Hills	El Centro Imp. Co.	CDMG
17	6.5	1987	Superstition Hills	Poe Road (temp)	USGS
18	7.0	1992	Cape Mendocino	Rio Dell Overpass	CDMG
19	7.6	1999	Chi-Chi, Taiwan	CHY101	CWB
20	7.6	1999	Chi-Chi, Taiwan	TCU045	CWB
21	6.6	1971	San Fernando	LA - Hollywood Stor	CDMG
22	6.5	1976	Friuli, Italy	Tolmezzo	--

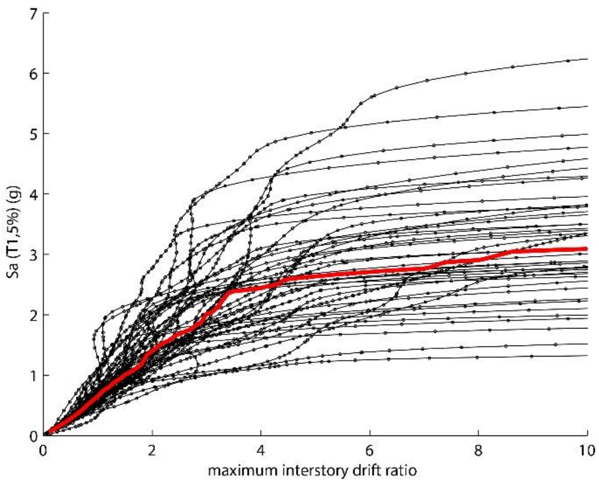

a) 5m bay length structure b) 8m bay length structure

Fig 5. comparison of IDA curves for 6-story structure.

to the table, difference between maximum and average Ω_0 is large for short period structures. The difference is at most 57% for short period structures and 13% for long period ones. Therefore, there is a significant difference between these two types of structures.

4. Incremental Dynamic Analysis

After determination of μ_T and Ω_0, an IDA [21] analysis must be carried out to calculate collapse margin ratio (CMR). IDA is an analysis method by which condition of structure can be traced from elastic to near collapse. For instance, Fig. 5 portrays the IDA curves of 6-story building (black lines). Median IDA curves are plotted by thick red lines, as well. It can be observed that 6-story building with 8m bay length is able to reach larger spectral accelerations. Thus, it is anticipated that this structure possesses larger collapse capacity. In the following, method of calculating CMR and adjusted CMR (ACMR) is provided:

First, spectral acceleration corresponding to maximum considered earthquake in the first period of structure ($\hat{S}_{\mathrm{MT}}$) is calculated. For short period structures

$$S_{MT} = S_{MS} \tag{7}$$

and for long period structures

$$S_{MT} = \frac{S_{M1}}{T} \tag{8}$$

Values of $S_{MS}$and S_{M1} are calculated by Eq. 6-1 of FEMA-P695. Response modification factor (R) is calculated by

$$R = \frac{S_{MT}}{1.5 \times C_S} \tag{9}$$

Where C_S is the design base shear coefficient. Table 2 highlights the R values of the aforementioned structures. Results show that the calculated values well correlate with R=8 suggested by ASCE/SEI 7-05. The difference of calculated values with code proposed values is only 7% in group D of long period structures.

Collapse margin ratio is determined by

$$CMR = \frac{\hat{S}_{\mathrm{CT}}}{\hat{S}_{\mathrm{MT}}} \tag{10}$$

$\hat{S}_{\mathrm{CT}}$ is the spectral acceleration at the point of collapse in median IDA curve.

Table 4. Summary of safety factors.

Group No.	Bay Details				Results			
	No. of stories	gravity loads	Bay length (m)	SDC	allowed ACMR	ACMR	Result	S.F. (%)
Group A								
01 – A	1	ordinary	5	D_{max}	1.52	3.18	accept	110
02 – A	2	ordinary	5	D_{max}	1.52	2.03	accept	33
03 – A	3	ordinary	5	D_{max}	1.52	2.07	accept	36
Mean of Performance Group					1.9	2.66	accept	40
Group B								
06 – B	6	ordinary	5	D_{max}	1.52	2.05	accept	35
09 – B	9	ordinary	5	D_{max}	1.52	2.4	accept	58
12 – B	12	ordinary	5	D_{max}	1.52	2.16	accept	42
15 – B	15	ordinary	5	D_{max}	1.9	2.07	accept	36
Mean of Performance Group					1.52	2.17	accept	14
Group C								
01 – C	1	ordinary	8	D_{max}	1.52	4.53	accept	198
02 – C	2	ordinary	8	D_{max}	1.52	4.09	accept	169
03 – C	3	ordinary	8	D_{max}	1.52	2.98	accept	94
Mean of Performance Group					1.9	3.85	accept	103
Group D								
06 – D	6	ordinary	8	D_{max}	1.52	2.58	accept	70
09 – D	9	ordinary	8	D_{max}	1.52	2.03	accept	33
12 – D	12	ordinary	8	D_{max}	1.52	2.89	accept	90
15 – D	15	ordinary	8	D_{max}	1.9	2.29	accept	51
Mean of Performance Group					1.52	2.45	accept	29

Collapse is defined by global instability in IDA curves and occurs when flat lines in IDA curves are observed. Since capacity of the structure and therefore CMR is dependent on the frequency content of the ground motion records, some modifications are needed. By applying a spectral shape factor (SSF_i), CMR is adjusted

$$ACMR_i = SSF_i \times CMR_i \tag{11}$$

SSF_i can be determined from Table 7-1 of FEMA-P695. Through applying the above methodology one can determine which structure can meet the desired performance levels. It is notable that using a Pass/Fail criteria is not an appropriate index for performance assessment since it gives no information about distance of structure condition from margins of allowed performance levels. In fact, by applying such approach no distinction can be made from structures with distance from marginal levels and the structures which are near the marginal levels. For this reason, a parameter is needed to define the factor of safety of a structure from performance levels. Margin of safety is defined as

$$(S.F)_i = \frac{ACMR_i - ACMR_{allowable}}{ACMR_{allowable}} \tag{12}$$

Table 4. summarizes the seismic performance of the structures as well as their factor of safety. In general, results reveal that all structures demonstrated an acceptable behavior during an earthquake. This confirms that ASCE/SEI 7-05 provisions lead to design of structures with appropriate margins of safety against collapse. In addition it indicates that elastic design methods considering R=8 result in acceptable nonlinear behavior of steel moment frames.

Moreover, pushover analysis results show that larger values of Ω were obtained for the structures. Therefore ASCE/SEI 7-05 by suggestion of Ω = 5 slightly underestimates the overstrength factor.

Table 5. S.F. based on period.

5m bay length			8m bay length	
No. of stories	T	S.F. (%)	T	S.F. (%)
1	0.31	110	0.28	198
2	0.56	33	0.45	169
3	0.69	36	0.56	94
6	1.03	35	0.88	70
9	1.43	58	1.37	33
12	1.60	42	1.52	90
15	1.98	36	1.79	51

Table 6. S.F. based on performance groups.

5m bay length		
Performance group	ACMR	S.F. (%)
Short Period	2.66	40
Long Period	2.17	14
8m bay length		
Performance group	ACMR	S.F. (%)
Short Period	3.85	103
Long Period	2.45	29

According to Figure 5, comparison of ACMR and SF values exhibits that for 8m bay length structures SF decreases from period T=0.28 to 1.37 and then abruptly increases up to T=1.52. From T=1.52 to T=1.79, SF decreases again. For 5m bay length structures, SF decreases from T=0.31 to T=1.03 and then increases up to T=1.43. For larger values of T, SF reduces again. Although variations of SF show large fluctuations, the variations for periods larger than 0.5 are much less. Table 6 displays summarized SFs for performance groups. For all cases, structures with 8m bay length exhibit a more desirable seismic performance since they reach larger ACMRs in comparison to structures with 5m bay length. This may be due to applying larger sections for larger bays which results in larger SF values. In summary, structures with short period show a better collapse capacity compared to larger period structures.

5. Conclusion

In this study, collapse capacity of a wide range of degrading steel moment frames was investigated. FEMA P-695 methodology was employed for analyses. By interpretation of static and dynamic nonlinear analyses, the following conclusions can be drawn

- By increase in height of the structure, the probability of collapse increases. However, the drop rate decreases with increase in height
- Overstrength factor provided by ASCE/SEI 7-05 is not always conservative. In this study, overstrength factors up to two times the suggested factor were obtained.
- Overstrength factor shows large variations. Therefore applying a single value in elastic analyses to model nonlinear behavior of a

wide range of structures will be an approximate.

- Structures with larger bay length demonstrate higher safety factor against collapse. This may be due to the fact that larger bay lengths result in higher design forces for the members which leads to larger sections. Therefore, these structures possess higher overstrength and consequently higher collapse safety factors.

REFERENCES

[1] Lignos, D., Krawinkler, H., (2012). ”Sidesway collapse of deterioration structural systems under seismic excitations” The John A. Blume Earthquake Engineering Center. Department of Civil and Environmental Engineering Stanford University.

[2] Jennings, P.C., Husid, R., (1968). “Collapse of yielding structures during earthquakes,” Journal of Engineering Mechanics, ASCE, Vol. 94, Issue 5, pp 1045-1065.

[3] Takizawa, H., Jennings, P., (1980) “Collapse of a model for ductile reinforced concrete frames under extreme earthquake motions,” Earthquake Engineering and Structural Dynamics, Vol. 8, Issue 2, pp: 117-144.

[4] Bernal, D., (1987). “Amplification factors for inelastic dynamic P-Delta effects in earthquake analysis,” Earthquake Engineering & Structural Dynamics, Vol. 15, Issue 5, pp: 635-651.

[5] Bernal, D., (1992). “Instability of buildings subjected to earthquakes,” Journal of Structural Engineering, ASCE, Vol. 118, Issue 8, pp: 2239-2260.

[6] Bernal, D., (1998). “Instability of buildings during seismic response,” Engineering Structures, Vol. 20, Issue 4-6, pp: 496-502.

[7] Rahnama, M. Krawinkler, H., (1993). “Effect of soft soils and hysteresis models on seismic design spectra,” John A. Blume Earthquake Engineering Research Center Report No. 108, Department of Civil Engineering, Stanford University.

[8] Miranda, E., Akkar, D., (2003). “Dynamic instability of simple structural systems.” Journal of Structural Engineering, ASCE, Vol. 129, Issue 12, pp: 1722–1726.

[9] Song, J., Pincheira, J., (2000). “Spectral displacement demands of stiffness and strength degrading systems,” Earthquake Spectra, Vol. 16, Issue 4, pp: 817-851, 2000.

[10] Ibarra, L.F., Medina, R.A., Krawinkler, H., (2002). “Collapse assessment of deteriorating SDOF systems,” Proceedings of the 12th European Conference on Earthquake Engineering, London, UK, Paper 665, Elsevier Science Ltd., September 9-13.

[11] Ibarra L.F., Medina R.A., Krawinkler H., (2005). “Hysteretic models that incorporate strength and stiffness deterioration,” Earthquake Engineering and Structural Dynamics, Vol. 34, Issue 12, pp: 1489-1511.

[12] Ibarra, L.F., Krawinkler, H., (2005). “Global collapse of frame structures under seismic excitations,” Report No. PEER 2005/06, Pacific Earthquake Engineering Research Center, University of California at Berkeley, Berkeley, California, 2005.

[13] FEMA-P695, (2009). “Quantification of building seismic performance factors,” prepared by the Applied Technology Council (ATC) for the Federal Emergency Management Agency (FEMA), Washington, DC.

[14] ASCE/SEI7–05, (2005), “Minimum Design Loads for Buildings and Other Structures”, American Society of Civil Engineers.

[15] BHRC, (2005), “Iranian code of practice for seismic resistance design of buildings: Standard no. 2800”. 3rd ed. Building and Housing Research Center.

[16] McKenna F, Feneves GL. (2009), “Open system for earthquake engineering

simulation (OpenSEES)", Version 2.1.0, Pacific Earthquake Engineering Research Center.

[17] Vamvasikos, D. and Cornell C.A., (2002). "Aplied Incremental Dynamic Analysis", 12th European Conference on Earthquake Engineering, London.

[18] Federal Emergency Management Agency; (2000). "Prestandard and Commentary for the Seismic Rehabilitation of Buildings", FEMA356, Washington, D.C.

[17] Ibarra L.F., Medina R.A., Krawinkler H., (2005), "Hysteretic models that incorporate strength and stiffness deterioration", Earthquake Engineering and Structural Dynamics, Vol. 34, Issue 12, pp: 1489-1511.

[18] Lignos, D.G., Krawinkler, H., (2011), "Deterioration modeling of steel components in support of collapse prediction of steel moment frames under earthquake loading", Journal of Structural Engineering, ASCE, Vol. 137, Issue 11, pp: 1291-1302.

[19] Steneker P. and Wiebe L., (2016), "Evaluation of THE contribution of panel zones to the global performance of moment resisting frames under seismic load", in proc. Canadian Society for Civil Engineering, London, 2016.

[20] Gupta, A., Krawinkler, H., (1999), "Prediction of seismic demands for SMRFs with ductileconnections and elements," SAC Background Document, Report No. SAC/BD-99/06, SAC Joint Venture, Sacramento, CA.

[21] Vamvatsikos D, Cornell CA., (2002). "Incremental dynamic analysis", Earthquake Engineering and Structural Dynamics; Vol. 31, Issue 3, pp: 491-514.